Dynamic gating in the nucleus accumbens: Behavioral state-dependent synchrony with the prefrontal cortex and hippocampus

Rifat J. Hussain[1]*, Aaron J. Gruber[1,2]* & Patricio O'Donnell[1,2,3]

[1] Center for Neuropharmacology and Neuroscience, Albany Medical College
[2] Department of Anatomy & Neurobiology, University of Maryland School of Medicine
[3] Department of Psychiatry, University of Maryland School of Medicine
* Co-first authors; contributed equally to this work

Running title: hippocampal-accumbens-prefrontal correlations

Corresponding Author: Patricio O'Donnell, MD, PhD
University of Maryland School of Medicine, Program in Neuroscience, Department of Anatomy & Neurobiology, 20 Penn St, room 251, Baltimore, MD 21201, phone: 410-706-6411, fax: 410-706-6410, email: podon002@umaryland.edu

Key words: Natural reward, local field potentials, accumbens, prefrontal cortex, hippocampus, electrophysiology

Figures: 6 Tables: 1 Supplementary Figures: 2

Words in summary: 145

Abstract

Contextual and sensory information, goals, and the motor plan to achieve them are integrated in the nucleus accumbens (NA). Although this integration needs flexibility to operate in a variety of environments, models of NA function rarely consider changing behavioral states. Here, intracellular recordings in anesthetized rats revealed rapid changes in the synchronization between NA up states and prefrontal cortical (PFC) local field potentials (LFPs). The synchronization of the NA with the PFC and ventral hippocampus also varied over time in awake rats, depending on the behavioral state of the animal: NA LFPs followed hippocampal theta rhythms during spatial exploration, but not during an operant task when they were instead synchronized with slower PFC rhythms. These data indicate that the ability of the NA to follow cortical inputs can rapidly change, allowing for a mechanism that could select an optimal response for a given behavioral condition.

The NA plays a central role in motivated, goal directed behaviors[1,2] and has been described as an interface between limbic and motor systems[3,4]. This brain region receives dense glutamatergic projections from the ventral hippocampus (VH)[5] and PFC[6], which converge on individual medium spiny neurons (MSNs)[7,8]. NA MSN action potential firing is driven by interactions between VH and PFC inputs[7], and the role of the NA on guiding behavior may depend on the composition of active NA neural assemblies determined by the state of afferent projections[9].

In anesthetized rats, VH inputs can gate PFC throughput in the NA[7]. Electrical VH stimulation evokes up states in NA neurons[7] and fornix or VH lesions eliminate these up states[7,10]. Furthermore, up state transitions in NA neurons are highly correlated with VH LFP and less correlated with PFC LFP[11]. These data suggest that synaptic inputs from the VH can drive up states in NA neuronal ensembles. Although there is evidence of hippocampal activity preceding NA cell firing with a delay consistent with monosynaptic responses in freely moving rats[12], the hippocampal gating

hypothesis has been developed in studies from anesthetized animals. In awake, freely moving animals it may be limited to certain hippocampal-dominated behavioral conditions. PFC stimulation was found to terminate up states[7] and this was interpreted as the PFC "closing the gate". If this scenario is correct, a strong correlation between NA and VH should be observed in awake animals, but epochs of strong PFC activity should disrupt NA-VH synchrony.

Here, we conducted *in vivo* intracellular recordings from anesthetized rats to assess variations in the synchrony between NA and cortical regions. Specifically, we sought to determine whether the synchrony between PFC activity and NA up states (reported to be weak[11]) could vary from event to event. We also recorded LFPs and single-unit activity simultaneously in the NA, VH and PFC in awake, freely moving rats using chronically implanted electrode arrays. LFPs were used as a measure of local network activity during two different behavioral conditions in the same session: first, when the rats were exploring the test chamber during the initial 10 minutes of recording; subsequently, in the same session the rats were required to press a lever in order to obtain a natural reward (sucrose). Cross-correlation of single-unit activity and the coherence between similar frequency peaks and bands in LFPs during spatial exploration and instrumental behavior were determined to assess whether the synchrony in electrical activity changed with the behavioral condition.

RESULTS

In vivo intracellular recordings

We tested whether active periods in the membrane potential of NA MSNs (up states) showed changes in their synchronization with PFC electrical activity. *In vivo* intracellular recordings from NA neurons were acquired simultaneously with LFPs from the PFC in anesthetized adult male Sprague-Dawley rats (n=13). NA neurons exhibited spontaneous transitions between a down state of -82.3 ± 4.2 mV and up states of -54.5 ± 2.6 mV (**Fig. 1a**). NA up states are known to be strongly

correlated with hippocampal LFPs but only weakly correlated with PFC fields when correlation is analyzed over long recording epochs[11]. We hypothesized that such weak correlation between NA up states and PFC LFPs could be the consequence of an *on* and *off* pattern (i.e., engaging during transitions to single up states) in anesthetized rats. To explore PFC-NA synchrony, we determined cross-covariance of membrane potential values in NA neurons with LFPs in the PFC (**Fig. 1a**) using a ±200 ms sliding window (**Fig 1b**). The covariance peaks typically corresponded to state transitions (**Fig. 1c**). Selecting cross-covariance analyses for only the times of transition to the up state in NA MSNs revealed that although many up state transitions co-varied with PFC LFPs, there were also NA state transitions that did not show covariance with PFC LFPs (**Fig. 1d**). In most NA neurons (8 of 10) the peak values of state transition-triggered cross covariance, as well as the value at zero lag, were significantly higher than cross covariance with randomized versions of the field potential ($p<0.01$; **Fig. 1e**; the randomization was done conservatively, preserving the near-1 Hz oscillation characteristic of anesthetized recordings). Thus, the extent of synchronization of NA MSN down and up states with PFC activity can change from one event to the next.

Does such transient synchronization reflect the ability of brief epochs of PFC activity to drive up states in NA MSNs? We tested this possibility by stimulating the PFC with a bursty pattern similar to what observed in awake rats during goal-directed behavior[13]. Unlike single-pulse stimulation[7], electrical stimulation of PFC with trains of pulses (5 pulses at 50 Hz) evoked sustained depolarizations similar to up states in anesthetized rats (n=5; **Fig. 2**). This suggests that high frequency PFC firing, such as what occurs during instrumental behavior, could exert a brief but powerful influence on NA activity.

Single-unit activity in NA, VH and PFC of awake rats

As the data presented above were collected in anesthetized rats, a condition in which cortical activity is strongly oscillatory[14] and in which we needed to drive the PFC with bursts of stimuli, it remained to be tested whether natural PFC activity in awake, behaving rats could overcome the

strong influence of hippocampal afferents on NA electrical activity. To assess this issue, we conducted multichannel extracellular recordings in six freely moving rats during a recording session that included an initial component of 5-15 minutes of exploratory behavior that was followed by instrumental behavior (bar pressing for sucrose reward). LFPs and single units were analyzed, and the rats' activity was monitored with a video camera to analyze epochs of recording that exhibited similar level of locomotion, and in which the rats were in front of the levers and fluid receptacle (for both the exploratory and instrumental behavior components). This was done to ensure the spatial and orientation information were similar in both conditions. The rats were tested during their active phase, as they had been housed with an inverted light-dark cycle.

During the instrumental task, firing rate was evaluated for a period comprising 10 sec prior to and 10 sec after the bar press for sucrose. A visual cue indicated availability of the reward, and rats typically pressed the lever within 1 or 2 seconds. NA (49/60), PFC (30/34) and VH (8/15) neurons exhibited previously described types of firing patterns relative to the lever press[15] (**Supplementary material; Table 1).** Crosscorrelograms were constructed to assess synchronization between different neurons across brain regions and whether it changed with the behavioral state. All NA-PFC pairs tested (n=8) showed enhanced correlation during the bar press compared to the exploratory period (**Fig. 3a**). The strength of the correlation was calculated by determining the ratio between crosscorrelogram peaks and shuffled crosscorrelograms. For NA-PFC pairs, this ratio was 1.33 ± 0.36 during the exploratory stage, and increased to 1.67 ± 0.40 during bar press (n=8; p=0.028). The correlation between NA and VH neurons did not differ between exploration and goal-directed behavior (1.60 ± 0.72 during exploration; 1.70 ± 0.70 during bar press; n=5; p>0.05; **Fig. 3b**). Thus, an operant task was associated with a stronger PFC-NA correlation in unit firing than spatial exploration.

Local field potentials in the NA, VH and PFC

LFPs were recorded simultaneously from the same wires that yielded single-unit data. Frequency components in this measure of population activity were determined using the Fast Fourier Transform. When the animals were allowed free exploration and the operant task had not yet been started, this analysis revealed a dominant 7-8 Hz (theta) peak in all three structures (**Fig. 4**). Theta oscillations are found in different mammalian structures but most prominently in the hippocampus[16], and are associated with complex behaviors like spatial exploration and memory functions[17-19]. During the operant task, the VH still exhibited a dominant theta peak, but the PFC and NA did not (**Fig. 4**). Both the PFC and NA exhibited dominant slow rhythms (in the delta range) during bar-pressing for a natural reward (**Fig. 4**). The delta band has been typically associated with slow-wave sleep[20,21], and it may contribute to the consolidation of memory traces acquired during the state of wakefulness[22]. However, evidence also supports a role for delta activity in awake animals. For example, low frequency components in monkey motor cortex can carry information about parameters of voluntary arm movement[23]. Furthermore, delta oscillations in humans increase significantly while performing the Wisconsin Card Sorting Test[24], which typically activates the PFC. In the NA, delta oscillations are highest in amplitude during the awake quiet state or during grooming[25]. Here, power spectra were also compared by calculating the relative power in different frequency bands. The primary differences between the two behavioral conditions in the recording session were increases in delta (1-4 Hz) oscillations in the PFC and NA during the instrumental behavior (**Fig. 5**); all frequency bands remained the same in the VH (**Fig. 5**). Thus, Thus, delta oscillations in the PFC and NA are important elements in the corticoaccumbens system when guided movement or response selection is needed, and were able to override the NA tight correlation with VH theta rhythms.

Next, we assessed synchronization of LFP activity among these regions in both components of the recording session. Co-spectral density, a measure of correlation of different frequency components, was calculated for LFPs simultaneously recorded from NA, PFC and VH, and it was used to determine coherence for the frequency values showing peaks in both spectra and in the co-

spectral analysis. This analysis provides a statistical measure of correlation (r^2). During exploratory activity, NA and VH LFPs exhibited a high coherence at 7.8 ± 0.5 Hz (r^2=0.93 ± 0.04; 18 pairs). A phase-lag analysis revealed that VH peaks in the theta range preceded identical peaks in the NA by 19 to 45 ms, suggesting that VH theta activity drives NA theta oscillations during spatial exploration. Such correlation between VH and NA theta peaks could not be observed during bar pressing for sucrose (**Fig. 6**), suggesting that hippocampal control of NA activity is weaker during goal-directed behaviors. The correlation between NA and PFC spectral peaks exhibited a different pattern. NA-PFC LFPs exhibited high coherence during bar press for sucrose (2.6 ± 0.8 Hz; r^2=0.94 ± 0.03; 20 pairs; **Fig. 6**). Phase-lag analysis revealed that PFC delta peaks preceded similar NA peaks by 9 to 24 ms. The data strongly suggest that NA follows VH activity during spatial exploration, but follows PFC activity during an operant task, even in the presence of similar spatial information. Thus, what seems to change between behavioral conditions is the link between NA and PFC, with strong PFC activation able to override the influence of VH inputs.

DISCUSSION

Temporal aspects of the correlation between NA activity and two of its major input sources were studied with *in vivo* intracellular recordings in anesthetized rats and multichannel recordings in awake rats. The correlation between NA up states and PFC field potentials can change from event to event, and burst-like stimulation of the PFC can elicit up states in NA neurons. Furthermore, LFPs and single unit activity in the NA, PFC, and VH changed with the behavioral state of the animal. When the rats were ambulating and not engaged in instrumental behavior, theta oscillations were prominent in all regions, but likely driven by the VH. The correlation between NA and VH was strong during exploration. However, during bar-pressing for a natural reward, delta oscillations became more prominent in the PFC and NA and the correlation between NA and PFC activity

increased. These results indicate that neuronal activity in the NA can be driven by different afferent systems, depending on the behavioral condition.

A hippocampal gating of NA activity had been proposed several years ago[7] and subsequent studies further supported this concept. For example, VH LFP were strongly correlated with up states in the NA[11]. Recordings in awake animals also revealed a robust VH-NA functional connectivity[12]. Here, we observed very strong theta oscillations in the NA, VH and PFC during spatial exploration, with VH theta preceding similar peaks in the PFC and NA. Thus, strong theta activity in the VH such as that observed during exploration is likely to drive a similar activity in the NA. In the instrumental behavior, however, the NA was better synchronized with the PFC, suggesting that during behaviors in which the PFC can become strongly activated, the hippocampal gating is overridden.

The high correlation between PFC and NA during lever pressing for reward at around 3 Hz was suggestive of PFC driving NA activity while VH activity remained the same. Indeed, phase-lag analyses revealed latencies consistent with a direct connection. The spectra observed in PFC and NA fields were not identical, however. In general, PFC fields presented several small peaks in the delta range whereas the NA exhibited a stronger single peak in that range. The NA peak was highly correlated with a same-frequency peak in the PFC, and the phase lag analysis was conducted between these two. Thus, the PFC to NA information may be narrowed by some sort of filtering occurring at the NA level, by which a specific frequency component is selected.

The increase in delta activity in the NA during goal-directed behavior takes place along with the loss of the theta peak, even though theta activity in the VH remains unchanged. As the recorded epochs for the spatial components were selected from periods in which the animal was in the same area of the box as when the goal-directed behavior was tested, VH place cells would be equally active in both conditions. So, more than a switch from spatial to goal-directed condition, the two states may represent the addition of a goal-directed state on top of steady spatial information. This could represent some extent of competition between spatial/contextual information (driven by

hippocampal afferents) and goals (driven by the PFC) in the NA. When goal information is critical for behavioral selection, electrical activity in the NA could disengage from a still active VH. It has indeed been shown in recordings from awake rats that NA neurons process place information, but their activation extends through a series of successive movements required to achieve a goal-directed behavior[26], suggesting that NA neurons can integrate VH spatial information with "goal-related" information. Thus, during conditions with strong PFC activity, PFC inputs to the NA may therefore override the influence of VH afferents and directly drive NA cells into a PFC-commanded pattern. Recent work from our lab indicates that burst PFC stimulation engages feed-forward inhibitory mechanisms in the NA (AJG, RJH and PO'D, Soc. Neurosci. Abstr., 2007), and it can be speculated they may be sufficient to shunt the response of NA neurons to VH inputs in the theta range.

The integration of information in the NA does depend on the behavioral state of the animal. It is therefore likely that during behavioral conditions in which the VH is strongly active (i.e., spatial exploration), the NA follows hippocampal commands and may serve to gate other cortical inputs[7]. Our *in vivo* data from anesthetized rats reveal that strong PFC activation with a bursty pattern similar to what has been reported during working memory tasks[27] can drive persistent depolarizations in the NA. Therefore, the NA could be envisioned as a critical relay station or switchboard that may determine the most appropriate behavioral output to the context and goals by selecting inputs that drive its activity according to the behavioral condition. A tight response to VH activity during VH-dependent behaviors and to the PFC during PFC-dependent behaviors could ensure that the relevant sets of commands are transferred through the ventral basal ganglia loops.

METHODS

All experiments were performed according to United States Public Health Service *Guide for the Care and Use of Laboratory Animals* and were approved by the Albany Medical College

Institutional Animal Care and Use Committee and the University of Maryland School of Medicine Institutional Animal Care and Use Committee.

***In vivo* intracellular recordings in anesthetized animals.** Intracellular recordings were conducted in 13 male Sprague Dawley rats (Charles River Laboratories, Wilmington, MA) weighing 260-430 g. Rats were initially anesthetized with chloral hydrate (400 mg/kg, i.p.), and subsequent anesthesia was maintained via constant infusion of chloral hydrate (20-30 mg/h, i.p.) using a syringe pump (Bioanalytical Systems, West Lafayette, IN). Body temperature was maintained at 36-38^{o}C using a heating pad and monitored with a rectal temperature probe (Fine Science Tools). Rats were placed in a stereotaxic apparatus (David Kopf), and an array of electrodes was implanted in the right prelimbic cortex (centroid of array tips with respect to bregma: 3.2 mm rostral and 0.6 mm lateral; depth: 4.3 mm ventral from skull; 30° angle toward midline). Electrode arrays were constructed with commercially available tungsten electrodes (WPI Inc., Sarasota, FL) or with 115 μm Teflon-coated tungsten wire (A-M Systems Inc., Carlsborg, WA). Electrode pairs were connected to a switchbox that allowed for the recording of cortical field potentials or delivery of electrical stimulation. Field potentials were amplified 1,000 times (DP-301 differential amplifier, Warner Instrument Corp., Hamden, CT), passed through a noise eliminator (Humbug, Quest Scientific Instr., Vancouver, Canada), digitized (Digidata 1322A, Axon Instruments, Union City, CA), band-pass filtered at 0.1-5 kHz, sampled at 10 kHz and recorded to hard drive using Axoscope software.

Intracellular recording electrodes were pulled from 1 mm (o.d.) borosilicate glass tubing (WPI) to a resistance of 40-100 MΩ with a P-97 Flaming-Brown microelectrode puller (Sutter Instruments, Novato, CA). Recording electrodes were filled with 2% Neurobiotin (Vector Laboratories, Burlingame, CA) in 2M potassium acetate and lowered into the right NA with a hydraulic microdrive (Trent Wells, Coulterville, CA) within the following range of coordinates: 1.3-1.7 mm rostral to bregma, 1.2-1.4 mm lateral to the midline, and 5.5-7.5 mm ventral from the cortical surface. Intracellular signals from the recording electrode were amplified (IR-283;

Neurodata, Delaware Water Gap, PA), low pass filtered at 2 kHz (FLA-01, Cygnus Tech. Inc., Delaware Water Gap, PA), digitized (Digidata 1322A, Axon Instruments), sampled at 10 KHz using Axoscope (Axon Instruments) and stored on a PC. Once a cell was impaled and the membrane potential stabilized, spontaneous fluctuations of membrane potential were recorded simultaneously with cortical field potentials, one at a time, from different cortical electrodes. The cortical electrode giving the best relationship with the activity of the recorded spiny neuron was used for analysis. In order for a cell to be included in the present data set, its resting membrane potential had to be more negative than -60 mV, its action potential amplitude greater than 40 mV measured from threshold, and input resistance greater than 35 MΩ.

Following electrophysiological recordings, Neurobiotin was injected into cells by passing positive current (0.5-1.0 nA, 200 ms pulses at 2 Hz) for 5-15 minutes through the recording electrode. At the completion of the experiments, rats were euthanized with an overdose of pentobarbital (100 mg/kg) and transcardially perfused with cold saline followed by cold 4% paraformaldehyde. Brains were postfixed in 4% paraformaldehyde for at least 24 h before being transferred to a solution of 30% sucrose in 0.1 M phosphate buffer for cryoprotection. Sections were cut (30-40 μm) using a freezing microtome and placed in phosphate buffer. Sections through the PFC were mounted on gelatin-coated slides and Nissl stained to verify placement of electrodes. Sections through the NA were processed for visualization of Neurobiotin-filled cells.

Traces of simultaneously recorded cortical LFP and intracellular NA neuron membrane potential were analyzed using native and custom-built functions implemented in Matlab (Mathworks, Natick, MA). First, up and down states were detected with a deadband threshold algorithm in which up states were defined as times in which the membrane potential exceeded an upper threshold and remained above a second lower threshold for at least 200 ms. The threshold varied from cell to cell, but was generally set near the middle of the voltage range between up and down states. Sliding window cross-covariance was computed for these time traces with a ±200 ms lag window and 5 ms time steps. Next, mean cross-covariance was computed over all transitions to

the up state and quantified by the distribution of magnitude and lag of their peaks. Statistical significance was determined by comparing distributions of those values with the distribution of cross-covariance computed in the same manner with surrogate traces. Surrogate trace sets were comprised of unaltered intracellular traces and randomized cortical field traces constructed by 1) computing the FFT of the signal, 2) randomizing the phases of the FFT, and 3) using inverse FFT to reconstruct a time series with the same spectral magnitudes but shuffled phases from the original cortical field trace. The Kolmogorov-Smirnov test was used to determine significance of cross covariance of data as compared to that of 50 iterations with randomized field traces.

Multichannel recordings in awake animals. Male Sprague Dawley rats (n=6) weighing between 300 and 375 g at the time of recording were obtained from Charles River Laboratories (Wilmington, MA). Each rat was housed individually in a reversed 12 hr dark/light cycle (on: 8 PM; off: 8 AM), so recordings were conducted during the animals' active phase. Water availability was restricted to 15 ml/day for 2-3 days prior and during the training, but rats had full access to food. Animals were maintained at no less than 85% of the pre-surgical body weight. Training sessions (30 min or 65 sucrose deliveries/day) were conducted in a Plexiglas chamber enclosed in a sound attenuating box (Med Associates, St. Albans, VT) provided with a fluid receptacle positioned 2 cm from the bottom of the chamber and 2 retractable levers on either side of the receptacle. Cue lights were 4 cm above the levers. Animals were trained on a fixed ratio 1 (FR1) to press a lever for sucrose reinforcement (50 μl/press). The training session started with turning on the house light and background white noise. Each trial started with the cue light and lever extension simultaneously. After a press, the lever retracted and sucrose was delivered. The task was not designed to assess working memory, but to ensure the animal was actively engaged in a reward-seeking activity. There was a 20 sec delay between trials. Experimental events were controlled and recorded using Med PC software from Med Associates. Once trained (>2.7 presses/min), rats had full access to water for 3-4 days prior to surgery.

The rats were anesthetized with ketamine (100 mg/kg, im) and xylazine (10 mg/kg, ip), and placed on a stereotaxic apparatus with non-puncturing ear bars (David Kopf instruments, Tujunga, CA). Body temperature was maintained at 36-38^{o}C using a heating pad and monitored with a rectal temperature probe (Fine Science Tools, Foster city, CA). Anesthesia was maintained by subsequent ketamine (20 mg/kg) and xylazine (2 mg/kg) injections every 60-90 min. Bupivacaine (0.25%) was applied subcutaneously before any skin incision was made. Small holes were drilled unilaterally in the skull to fit linear 1x8 or square 2x3x3 microelectrode arrays (NB Labs, Denison, TX). Seven rats had microelectrodes implanted in the PFC, NA and VH (**Suppl. Fig. 1**). The coordinates[28] for the NA were: 1.4-1.6 mm rostral to bregma (AP), 0.5-2.5 mm from midline (ML) and 7.0-7.5 mm from skull surface (DV). For the VH, they were (in mm): -4.8-5.6 AP, 3.5 ML and 7.0-8.0 DV; for the PFC, they were 2.8-3.5 AP, 0.5-1 ML and 4-4.5 DV. Five to six additional holes were made for ground wires and screws to anchor all the implants with dental cement. At the end of the surgery each rat received 5 mg/kg of diazepam (ip) and enrofloxazine (2.3 mg/kg, ip), as well as 12-15 ml of saline (sc). Antibiotic ointment was applied topically around the implant for 2-3 days. Rats were given 1-2 weeks for full recovery before starting the recording sessions.

Simultaneous LFP and single unit recordings were conducted using a multichannel acquisition processor (MAP; Plexon Inc., Dallas TX). Single unit data were acquired at 40 kHz. Field potential data were acquired at 1 kHz using a National Instruments AD card (NIDAQ). Headstages were connected to a lightweight cable attached to the Plexon recording system via a commutator. Online isolation and discrimination of neuronal activity was acquired using the MAP system. Selected waveforms that exceeded the amplitude threshold (3 SD above noise) were time-stamped and stored for subsequent offline analyses using offline sorter (Plexon). For field potentials, data were analyzed offline using Neuroexplorer (Plexon). Behavioral events (lever extension, lever press, sucrose delivery and reward entry) were also monitored and recorded using the data acquisition software.

LFP and single unit data were acquired over 4-6 recording sessions for each animal, during a period of 2-4 weeks starting about 2 weeks after surgery. The spatial exploration data were collected 5-10 min after the rat was placed in the chamber. For LFP, ten-second epochs were selected, ensuring they included ambulatory activity near the levers and water receptacle. Goal-directed data were collected after ten initial sucrose reinforcements. Ten-second epochs were selected, and they included the cue, bar press, reward delivery and a few seconds preceding and subsequent to these events. Power spectral density data were analyzed in Neuroexplorer and Statistica (Tulsa, OK). Four microwires with confirmed histology were selected from each structure in every rat. For each microwire, 2-3 different recording sessions were analyzed. Power spectral densities were summed over the range of 1-4 Hz (delta), 4-8 Hz (theta), 8-14 Hz (alpha), 14-30 Hz (beta) and 30-50 Hz (gamma) to compare spectral bands during exploration and bar press. Cross-spectral density was calculated with *Statistica* using a Hamming window as previously reported[11, 29]. Coherence between similar-frequency peaks in the individual spectra was calculated by standardizing the cross-amplitude values. Cross-spectral densities were squared and divided by the product of spectral densities of each recording. The result was interpreted as a squared correlation coefficient (r^2) for statistical purposes. High coherence values (>0.75) were taken as indicators of oscillatory activity at that particular frequency being synchronized.

Single-unit data were analyzed using Neuroexplorer. Principal component analysis along several waveform components was used to separate individual units in the recordings. Units were only considered if they were at least 3 times higher than background noise activity (peak-to-peak). Changes in firing rate of individual neurons were plotted in peri-event histograms along with raster plots where the bar press were used as reference. To determine the cross-correlation among single units, PFC-NA and VH-NA, crosscorrelograms were plotted using Neuroexplorer during exploration and bar press over 4 sec periods (bin size=10 ms).

At the end of the final recording session, animals were deeply anesthetized with sodium pentobarbital (100 mg/kg). In order to mark the recording sites, 10-20 μA current was passed for 5-

10 sec in selected wires to deposit iron. Animals were transcardially perfused with ice-cold saline followed by formalin solution, and brains were removed and post fixed in formalin for at least 24 hr. Serial 40-50 μm coronal sections were cut through the PFC, NA, and VH using a freezing microtome, and mounted on gelatin-coated slides. All sections were Nissl-stained, counterstained with Prussian blue (5% potassium ferricyanide in 10% HCl) for electrode tip placement, cover slipped in Permount and examined on an Olympus microscope (CH30, Tokyo, Japan) using the Paxinos and Watson atlas (1998) for reference. Electrode placements were confirmed and only data from wires with confirmed placement were used in the analyses.

ACKNOWLEDGEMENTS

We thank Ms. Gwendolyn Calhoon for her technical assistance and Dr. Geoffrey Schoenbaum, Dr. Regina Carelli, Dr. Carrie E. John and Ms. Kathy Toreson for helpful comments on an earlier version of the manuscript. This work was supported by USPHS grant MH60131 (PO'D) and a grant from the Tourette's Syndrome Association (AJG). The authors have no conflict of interest to disclose.

AUTHOR CONTRIBUTION

RJH conducted the recordings in awake rats; AJG carried out the intracellular recordings; PO'D designed the study, supervised the project and wrote the manuscript.

Table 1. Different types of phasic and non-phasic neurons in NA, PFC and VH.

	RFe	RFi	PR	PR+RF	NR	Total
NA	31 (52%)	8 (13%)	6 (10%)	4 (7%)	11 (18%)	60
PFC	11 (32%)	11 (32%)	5 (15%)	3 (9%)	4 (12%)	34
VH	8 (53%)	0	0	0	7 (47%)	15

REFERENCES

1. Kelley, A. E. Ventral striatal control of appetitive motivation: role in ingestive behavior and reward-related learning. *Neurosci Biobehav Rev* **27**, 765-776 (2004).
2. Wise, R. A. Dopamine, learning and motivation. *Nat Rev Neurosci* **5**, 483-94 (2004).
3. Mogenson, G. J., Jones, D. L. & Yim, C. Y. From motivation to action: functional interface between limbic system and the motor system. *Progr. Neurobiol.* **14**, 69-97 (1980).
4. Groenewegen, H. J., Wright, C. I. & Beijer, A. V. J. The nucleus accumbens: gateway for limbic structures to reach the motor system? *Progr. Brain Res.* **107**, 485-511 (1996).
5. Kelley, A. E. & Domesick, V. B. The distribution of the projection from the hippocampal formation to the nucleus accumbens in the rat: an anterograde- and retrograde-horseradish peroxidase study. *Neuroscience* **7**, 2321-2335 (1982).
6. Berendse, H. W., Galis-de Graaf, Y. & Groenewegen, H. J. Topographical organization and relationship with ventral striatal compartments of prefrontal corticostriatal projections in the rat. *J. Comp. Neurol.* **316**, 314-347 (1992).
7. O'Donnell, P. & Grace, A. A. Synaptic interactions among excitatory afferents to nucleus accumbens neurons: hippocampal gating of prefrontal cortical input. *J. Neurosci.* **15**, 3622-3639 (1995).
8. French, S. J. & Totterdell, S. Hippocampal and prefrontal cortical inputs monosynaptically converge with individual projection neurons of the nucleus accumbens. *J Comp Neurol* **446**, 151-165. (2002).
9. O'Donnell, P. Ensemble coding in the nucleus accumbens. *Psychobiology* **27**, 187-197 (1999).
10. Goto, Y. & O'Donnell, P. Delayed mesolimbic system alteration in a developmental animal model of schizophrenia. *J Neurosci* **22**, 9070-9077 (2002).
11. Goto, Y. & O'Donnell, P. Synchronous activity in the hippocampus and nucleus accumbens in vivo. *J Neurosci* **21**, RC131. (2001).
12. Tabuchi, E. T., Mulder, A. B. & Wiener, S. I. Position and behavioral modulation of synchronization of hippocampal and accumbens neuronal discharges in freely moving rats. *Hippocampus* **10**, 717-728 (2000).
13. Peters, Y. M., O'Donnell, P. & Carelli, R. M. Prefrontal cortical cell firing during maintenance, extinction, and reinstatement of goal-directed behavior for natural reward. *Synapse* **56**, 74-83 (2005).
14. Steriade, M., Nunez, A. & Amzica, F. Intracellular analysis of relations between the slow (< 1 Hz) neocortical oscillation and other sleep rhythms of the electroencephalogram. *J Neurosci* **13**, 3266-83 (1993).
15. Carelli, R. M. Nucleus accumbens cell firing during goal-directed behaviors for cocaine vs. 'natural' reinforcement. *Physiol Behav* **76**, 379-87 (2002).
16. Buzsaki, G. Theta oscillations in the hippocampus. *Neuron* **33**, 325-40 (2002).
17. Caplan, J. B. et al. Human theta oscillations related to sensorimotor integration and spatial learning. *J Neurosci* **23**, 4726-36 (2003).
18. Buzsaki, G. Theta rhythm of navigation: link between path integration and landmark navigation, episodic and semantic memory. *Hippocampus* **15**, 827-40 (2005).

19. Vertes, R. P. Hippocampal theta rhythm: a tag for short-term memory. *Hippocampus* **15**, 923-35 (2005).
20. Steriade, M., Nuñez, A. & Amzica, F. A novel slow (<1 Hz) oscillation of neocortical neurons in vivo: depolarizing and hyperpolarizing components. *J. Neurosci.* **13**, 3252-3265 (1993).
21. Mahon, S. et al. Distinct patters of striatal medium spiny neuron activity during the natural sleep-wake cycle. *J Neurosci* **26**, 12587-12595 (2006).
22. Steriade, M. & Amzica, F. Coalescence of sleep rhythms and their chronology in corticothalamic networks. *Sleep Res Online* **1**, 1-10 (1998).
23. Rickert, J. et al. Encoding of movement direction in different frequency ranges of motor cortical local field potentials. *J Neurosci* **25**, 8815-24 (2005).
24. Gonzalez-Hernandez, J. A. et al. Wisconsin Card Sorting Test synchronizes the prefrontal, temporal and posterior association cortex in different frequency ranges and extensions. *Hum Brain Mapp* **17**, 37-47 (2002).
25. Leung, L. S. & Yim, C. Y. Rhythmic delta-frequency activities in the nucleus accumbens of anesthetized and freely moving rats. *Can J Physiol Pharmacol* **71**, 311-20 (1993).
26. Mulder, A. B., Tabuchi, E. & Wiener, S. I. Neurons in hippocampal afferent zones of rat striatum parse routes into multi-pace segments during maze navigation. *Eur J Neurosci* **19**, 1923-32 (2004).
27. Chafee, M. V. & Goldman-Rakic, P. S. Matching patterns of activity in primate prefrontal area 8a and parietal area 7ip neurons during a spatial working memory task. *J Neurophysiol* **79**, 2919-40 (1998).
28. Paxinos, G. & Watson, C. The rat brain in stereotaxic coordinates (Academic Press, San Diego, 1998).
29. Goto, Y. & O'Donnell, P. Network synchrony in the nucleus accumbens in vivo. *J Neurosci* **21**, 4498-4504. (2001).
30. Chang, J.-Y., Zhang, L., Janak, P. H. & Woodward, D. J. Neuronal responses in prefrontal cortex and nucleus accumbens during heroin self-administration in freely moving rats. *Brain Res.* **754**, 12-20 (1997).

Figure legends

Figure 1 Cross-covariance analysis of intracellular NA neuron membrane potential and PFC LFP in anesthetized rats. (**a**) Simultaneous recording of intracellular membrane potential of a NA medium spiny neuron (MSN; top) and PFC field potential (LFP; bottom) showing spontaneous oscillations typical of an anesthetized rat. Transitions of MSN membrane potential between a hyperpolarized down state and depolarized up states are detected with a threshold (dotted line). (**b**) Pseudocolor plot of the cross covariance of these traces with a ±200 ms time lag window (ordinate). MSN membrane potential transitions from down to up states are indicated by dark triangles, and up to down transitions with white triangles. This panel shows only a portion of the recorded trace; analyses in subsequent panels include the full traces. Oblique arrows point to two consecutive up state onsets showing high covariance (left) and no covariance (right) with PFC LFP. (**c**) Overlay of the cross covariance plot in **b** and the MSN membrane potential trace in **a** showing the high covariance epochs to correspond to state transitions. (**d**) Cross covariance at successive down-to-up state transitions from data in **a**, showing that both the magnitude and lag of the peak cross-covariance (indicated by '+') vary in time. Transitions that co-vary with PFC LFP are interspersed with those that do not co-vary. (**e**) Cross covariance in **b** plotted in time and superimposed with mean ± standard deviation of cross covariance computed from randomized versions of the traces in **a** (gray region). Cross-covariance near lag=0 shows the data clustered in two populations: a significantly covariant set of events and others with almost no covariance.

Figure 2 PFC stimulation with trains of pulses evokes persistent depolarizations in NA neurons. Overlay of six traces obtained from a NA neuron during *in vivo* intracellular recording from an anesthetized rat, showing the membrane potential responses to stimulating the PFC with a train of 5 pulses at 50 Hz (arrows indicate the stimulation times; stimulus artifacts were removed for clarity).

The traces were selected to display stimuli delivered during both up and down states, and in either case a sustained depolarization was observed.

Figure 3 PFC-NA unit correlation is strengthened during bar press for a natural reward. (**a**) Representative cross-correlograms of a NA-PFC neuron pair (referenced to PFC firing at time 0) when the animal was exploring (gray bars) and during bar pressing for sucrose (black bars). Right: bar graphs showing the ratio between the crosscorrelogram peak and a similar analysis of shuffled recordings from the same pairs for both behavioral conditions. Mean ± SD; * $p<0.05$. (**b**) Similar cross-correlation of a representative VH-NA pair during spatial exploration (gray) and bar pressing (red). No differences were observed in these cases.

Figure 4 Dominant frequency peaks in VH, NA and PFC field potentials during exploration and during bar pressing for a natural reward. (**a**) Representative LFP traces from a microelectrode in the VH during exploration (left) and bar press (right). The arrows on the top indicate cue presentation (left) and bar press (right). Calibration bars are at the bottom. Bottom: Normalized spectral density (expressed as % for each bin of the total power in the 1-50 Hz range) obtained from the trace shown above. Left histogram shows power spectrum during exploring and the right histogram shows spectrum during bar pressing in the same session. Insets show overlaid spectra from 4 different microelectrodes for low (0-10 Hz) frequencies. Strong theta peaks are evident in the VH in both behavioral conditions. (**b**) Similar display of representative NA traces revealing a dominant theta peak during exploration and a dominant delta peak during goal-directed behavior. (**c**) Representative traces and spectral density histograms from PFC field potentials also showing dominant theta activity during ambulation and delta peaks during goal directed behavior.

Figure 5 Weight of spectral bands during spatial exploration and goal-directed behavior. Bar graphs depicting summed power for the 1-4 Hz (delta), 4-8 Hz (theta), 8-14 Hz (alpha), 14-30 (beta), and 30-50 (gamma) bands. Gray bars show the weight of each band during spatial exploration and black bars represent band weight during goal-directed behavior. Top to bottom graphs illustrate spectral bands from all accumbens, hippocampal, and PFC recordings.

Figure 6 Spectral density and coherence analyses of NA-VH fields and NA-PFC fields during exploration and goal-directed behavior. Cross-spectral densities were calculated to determine coherence between similar frequency peaks in LFP obtained simultaneously from different brain regions. Top left: Overlay of co-spectral data from two different NA-VH pairs simultaneously recorded while the animal was exploring, revealing a high coherence in the theta range (r^2 value shown on top of peak). Top right: Co-spectral histograms from the same pairs in the same session but recorded while the animal was bar pressing for sucrose, revealing a lack of correlation. Bottom left: Overlay of co-spectral density histograms from two NA-PFC pairs recorded simultaneously while the animal was exploring, revealing weak peaks at both the delta and theta frequencies. Bottom right: Co-spectral density histograms from the same pairs of recordings in the same session but while the animal was bar pressing for sucrose, revealing high coherence at a delta peak.

Supplementary Material. Firing patterns in freely moving rats.

Most NA neurons (52%) exhibited an increase in firing following lever press (type reinforcement-excitation (RFe); n=31; **Suppl. Fig. 1a**); 13% exhibited a decrease (type reinforcement-inhibition (RFi); n=8; **Suppl. Fig. 1b**); and 10% exhibited increases in firing rate preceding the lever press (i.e., between the cue and lever press; type pre-response (PR); n=6; **Suppl. Fig. 1c**). A small number (7%) of neurons exhibited a dual response (type PR+RF; n=4). The remaining 18% neurons did not change firing during the reinforced response (non-phasic cells; n=11). PFC neurons

exhibited similar response patterns, as reported previously[13, 30]; they could also be classified as PR (15%; n=5), RFe (32%; n=11), RFi (32%; n=11) or PR+RF (9%; n=3). The remaining four PFC neurons (12%) did not show any change in firing rate. In the VH, almost half of the neurons (53%; n=8) exhibited the RFe pattern and 47% (n=7) of the neurons did not show any change in firing rate.

Histological confirmation of microelectrode tracks

Representative coronal Nissl-stained sections were used to identify electrode tracks and recording sites in the PFC, NA and VH (**Suppl. Fig. 2**). The squared areas are zoomed and enlarged horizontally to illustrate the end of electrode tracks (arrowheads). Numbers indicate the distance to bregma in mm.

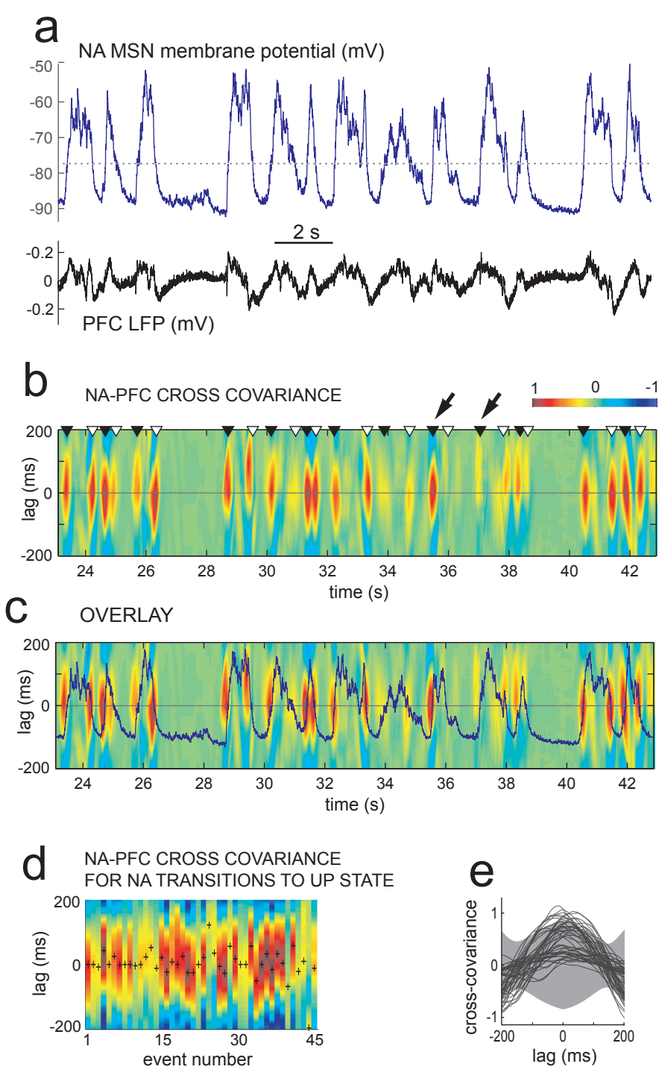

Hussain, Gruber, O'Donnell
Figure 1

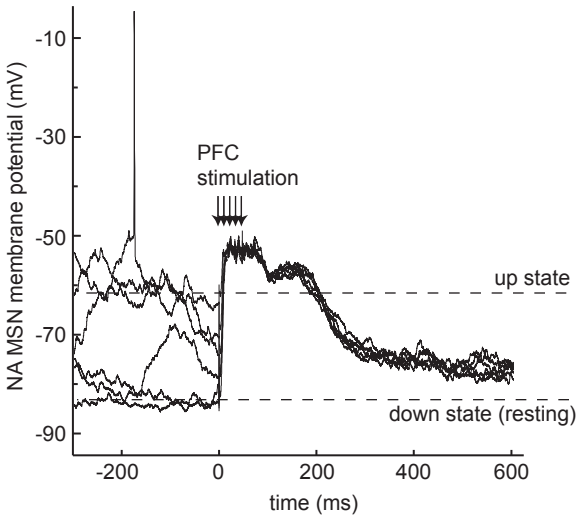

Hussain, Gruber, O'Donnell
Figure 2

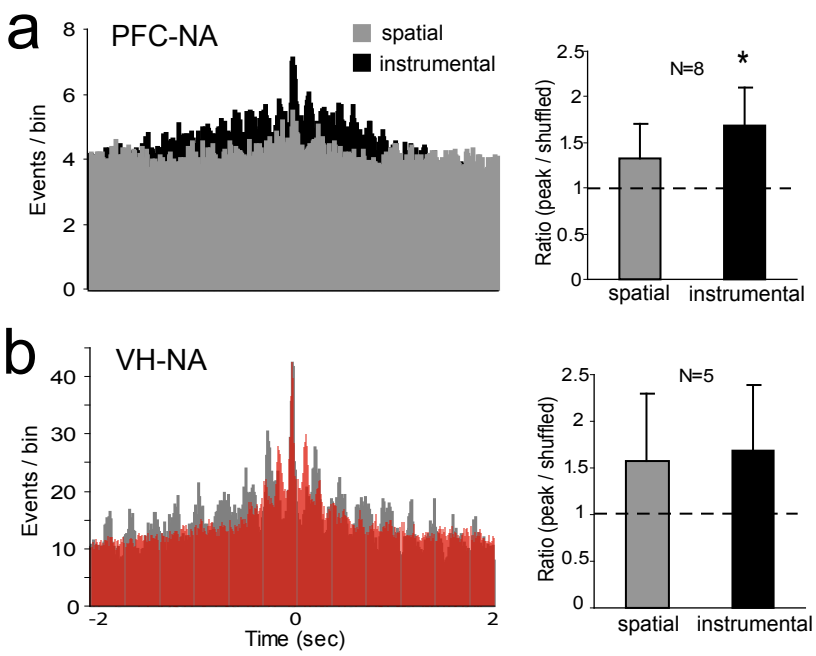

Hussain, Gruber, O'Donnell
Figure 3

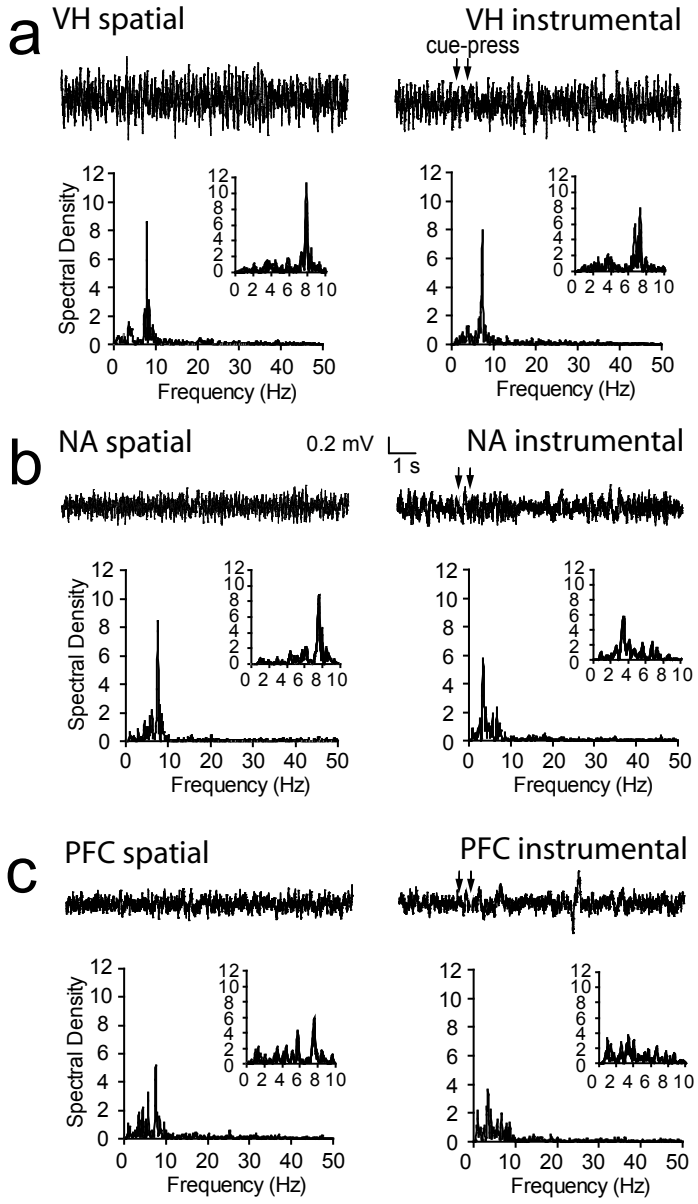

Hussain, Gruber, O'Donnell
Figure 4

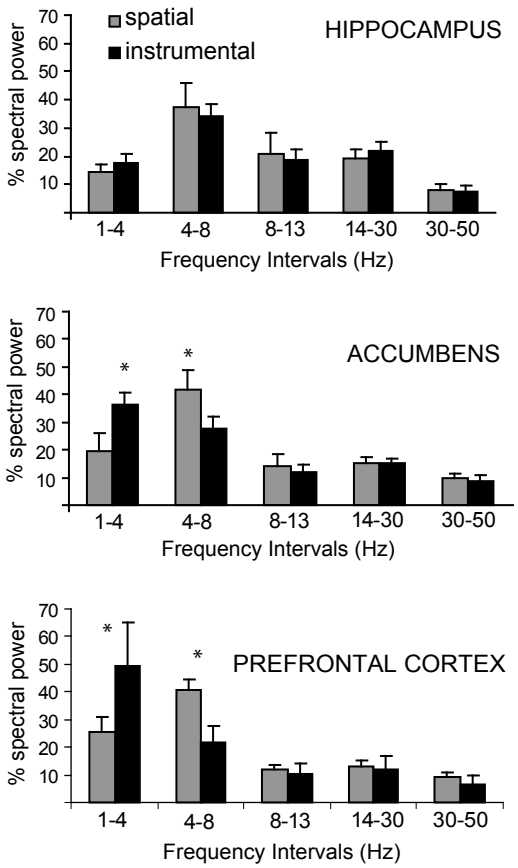

Hussain, Gruber, O'Donnell
Figure 5

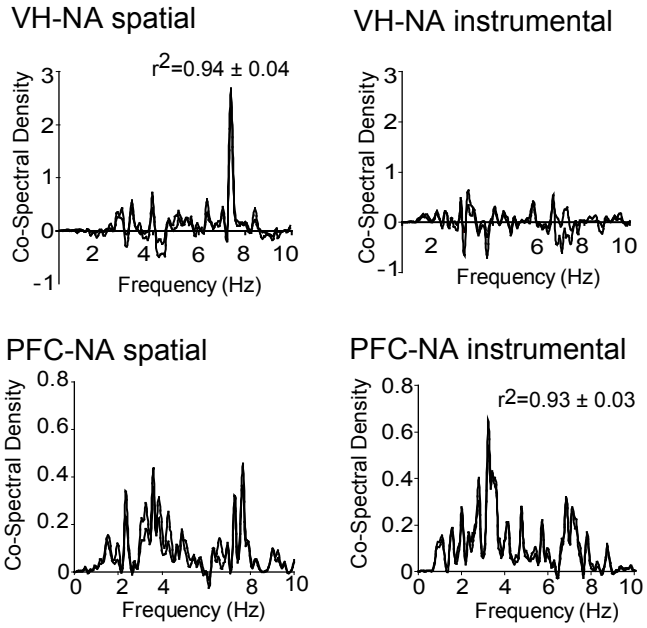

Hussain, Gruber, O'Donnell
Figure 6